

MIT Open Access Articles

Search for CP violation in the decays $D^{\pm} \rightarrow K_S^0 K^{\pm}$, $D_s^{\pm} \rightarrow K_S^0 K^{\pm}$, and $D_s^{\pm} \rightarrow K_S^0 \pi^{\pm}$

The MIT Faculty has made this article openly available. **Please share** how this access benefits you. Your story matters.

Citation: Lees, J. P. et al. "Search for CP Violation in the Decays $D^{\pm} \rightarrow K_S^0 K^{\pm}$, $D_s^{\pm} \rightarrow K_S^0 K^{\pm}$, and $D_s^{\pm} \rightarrow K_S^0 \pi^{\pm}$." Physical Review D 87.5 (2013). © 2013 American Physical Society

As Published: <http://dx.doi.org/10.1103/PhysRevD.87.052012>

Publisher: American Physical Society

Persistent URL: <http://hdl.handle.net/1721.1/81236>

Version: Final published version: final published article, as it appeared in a journal, conference proceedings, or other formally published context

Terms of Use: Article is made available in accordance with the publisher's policy and may be subject to US copyright law. Please refer to the publisher's site for terms of use.



Search for CP violation in the decays $D^\pm \rightarrow K_S^0 K^\pm$, $D_s^\pm \rightarrow K_S^0 K^\pm$, and $D_s^\pm \rightarrow K_S^0 \pi^\pm$

J. P. Lees,¹ V. Poireau,¹ V. Tisserand,¹ E. Grauges,² A. Palano,^{3a,3b} G. Eigen,⁴ B. Stugu,⁴ D. N. Brown,⁵ L. T. Kerth,⁵
 Yu. G. Kolomensky,⁵ G. Lynch,⁵ H. Koch,⁶ T. Schroeder,⁶ D. J. Asgeirsson,⁷ C. Hearty,⁷ T. S. Mattison,⁷
 J. A. McKenna,⁷ R. Y. So,⁷ A. Khan,⁸ V. E. Blinov,⁹ A. R. Buzykaev,⁹ V. P. Druzhinin,⁹ V. B. Golubev,⁹
 E. A. Kravchenko,⁹ A. P. Onuchin,⁹ S. I. Serednyakov,⁹ Yu. I. Skovpen,⁹ E. P. Solodov,⁹ K. Yu. Todyshev,⁹
 A. N. Yushkov,⁹ D. Kirkby,¹⁰ A. J. Lankford,¹⁰ M. Mandelkern,¹⁰ B. Dey,¹¹ J. W. Gary,¹¹ O. Long,¹¹ G. M. Vitug,¹¹
 C. Campagnari,¹² M. Franco Sevilla,¹² T. M. Hong,¹² D. Kovalskyi,¹² J. D. Richman,¹² C. A. West,¹² A. M. Eisner,¹³
 W. S. Lockman,¹³ A. J. Martinez,¹³ B. A. Schumm,¹³ A. Seiden,¹³ D. S. Chao,¹⁴ C. H. Cheng,¹⁴ B. Echenard,¹⁴
 K. T. Flood,¹⁴ D. G. Hitlin,¹⁴ P. Ongmongkolkul,¹⁴ F. C. Porter,¹⁴ A. Y. Rakitin,¹⁴ R. Andreassen,¹⁵ Z. Huard,¹⁵
 B. T. Meadows,¹⁵ M. D. Sokoloff,¹⁵ L. Sun,¹⁵ P. C. Bloom,¹⁶ W. T. Ford,¹⁶ A. Gaz,¹⁶ U. Nauenberg,¹⁶ J. G. Smith,¹⁶
 S. R. Wagner,¹⁶ R. Ayad,^{17,*} W. H. Toki,¹⁷ B. Spaan,¹⁸ K. R. Schubert,¹⁹ R. Schwierz,¹⁹ D. Bernard,²⁰ M. Verderi,²⁰
 P. J. Clark,²¹ S. Playfer,²¹ D. Bettoni,^{22a} C. Bozzi,^{22a} R. Calabrese,^{22a,22b} G. Cibinetto,^{22a,22b} E. Fioravanti,^{22a,22b}
 I. Garzia,^{22a,22b} E. Luppi,^{22a,22b} L. Piemontese,^{22a} V. Santoro,^{22a} R. Baldini-Ferroli,²³ A. Calcaterra,²³ R. de Sangro,²³
 G. Finocchiaro,²³ P. Patteri,²³ I. M. Peruzzi,^{23,†} M. Piccolo,²³ M. Rama,²³ A. Zallo,²³ R. Contri,^{24a,24b} E. Guido,^{24a,24b}
 M. Lo Vetere,^{24a,24b} M. R. Monge,^{24a,24b} S. Passaggio,^{24a} C. Patrignani,^{24a,24b} E. Robutti,^{24a} B. Bhuyan,²⁵ V. Prasad,²⁵
 M. Morii,²⁶ A. Adametz,²⁷ U. Uwer,²⁷ H. M. Lacker,²⁸ T. Lueck,²⁸ P. D. Dauncey,²⁹ U. Mallik,³⁰ C. Chen,³¹
 J. Cochran,³¹ W. T. Meyer,³¹ S. Prell,³¹ A. E. Rubin,³¹ A. V. Gritsan,³² N. Arnaud,³³ M. Davier,³³ D. Derkach,³³
 G. Grosdidier,³³ F. Le Diberder,³³ A. M. Lutz,³³ B. Malaescu,³³ P. Roudeau,³³ M. H. Schune,³³ A. Stocchi,³³
 G. Wormser,³³ D. J. Lange,³⁴ D. M. Wright,³⁴ J. P. Coleman,³⁵ J. R. Fry,³⁵ E. Gabathuler,³⁵ D. E. Hutchcroft,³⁵
 D. J. Payne,³⁵ C. Touramanis,³⁵ A. J. Bevan,³⁶ F. Di Lodovico,³⁶ R. Sacco,³⁶ M. Sigamani,³⁶ G. Cowan,³⁷
 D. N. Brown,³⁸ C. L. Davis,³⁸ A. G. Denig,³⁹ M. Fritsch,³⁹ W. Gradl,³⁹ K. Griessinger,³⁹ A. Hafner,³⁹ E. Prencipe,³⁹
 R. J. Barlow,^{40,‡} G. D. Lafferty,⁴⁰ E. Behn,⁴¹ R. Cenci,⁴¹ B. Hamilton,⁴¹ A. Jawahery,⁴¹ D. A. Roberts,⁴¹
 C. Dallapiccola,⁴² R. Cowan,⁴³ D. Dujmic,⁴³ G. Sciolla,⁴³ R. Cheaib,⁴⁴ P. M. Patel,^{44,§} S. H. Robertson,⁴⁴
 P. Biassoni,^{45a,45b} N. Neri,^{45a} F. Palombo,^{45a,45b} L. Cremaldi,⁴⁶ R. Godang,^{46,||} R. Kroeger,⁴⁶ P. Sonnek,⁴⁶
 D. J. Summers,⁴⁶ X. Nguyen,⁴⁷ M. Simard,⁴⁷ P. Taras,⁴⁷ G. De Nardo,^{48a,48b} D. Monorchio,^{48a,48b} G. Onorato,^{48a,48b}
 C. Sciacca,^{48a,48b} M. Martinelli,⁴⁹ G. Raven,⁴⁹ C. P. Jessop,⁵⁰ J. M. LoSecco,⁵⁰ K. Honscheid,⁵¹ R. Kass,⁵¹ J. Brau,⁵²
 R. Frey,⁵² N. B. Sinev,⁵² D. Strom,⁵² E. Torrence,⁵² E. Feltresi,^{53a,53b} N. Gagliardi,^{53a,53b} M. Margoni,^{53a,53b}
 M. Morandin,^{53a} A. Pompili,^{53a} M. Posocco,^{53a} M. Rotondo,^{53a} G. Simi,^{53a} F. Simonetto,^{53a,53b} R. Stroili,^{53a,53b}
 S. Akar,⁵⁴ E. Ben-Haim,⁵⁴ M. Bomben,⁵⁴ G. R. Bonneaud,⁵⁴ H. Briand,⁵⁴ G. Calderini,⁵⁴ J. Chauveau,⁵⁴ O. Hamon,⁵⁴
 Ph. Leruste,⁵⁴ G. Marchiori,⁵⁴ J. Ocariz,⁵⁴ S. Sitt,⁵⁴ M. Biasini,^{55a,55b} E. Manoni,^{55a,55b} S. Pacetti,^{55a,55b}
 A. Rossi,^{55a,55b} C. Angelini,^{56a,56b} G. Batignani,^{56a,56b} S. Bettarini,^{56a,56b} M. Carpinelli,^{56a,56b,¶} G. Casarosa,^{56a,56b}
 A. Cervelli,^{56a,56b} F. Forti,^{56a,56b} M. A. Giorgi,^{56a,56b} A. Lusiani,^{56a,56c} B. Oberhof,^{56a,56b} E. Paoloni,^{56a,56b} A. Perez,^{56a}
 G. Rizzo,^{56a,56b} J. J. Walsh,^{56a} D. Lopes Pegna,⁵⁷ J. Olsen,⁵⁷ A. J. S. Smith,⁵⁷ F. Anulli,^{58a} R. Faccini,^{58a,58b}
 F. Ferrarotto,^{58a} F. Ferroni,^{58a,58b} M. Gaspero,^{58a,58b} L. Li Gioi,^{58a} M. A. Mazzoni,^{58a} G. Piredda,^{58a} C. B nger,⁵⁹
 O. Gr nberg,⁵⁹ T. Hartmann,⁵⁹ T. Leddig,⁵⁹ C. Vo ,⁵⁹ R. Waldi,⁵⁹ T. Adye,⁶⁰ E. O. Olaiya,⁶⁰ F. F. Wilson,⁶⁰
 S. Emery,⁶¹ G. Hamel de Monchenault,⁶¹ G. Vasseur,⁶¹ Ch. Y che,⁶¹ D. Aston,⁶² D. J. Bard,⁶² J. F. Benitez,⁶²
 C. Cartaro,⁶² M. R. Convery,⁶² J. Dorfan,⁶² G. P. Dubois-Felsmann,⁶² W. Dunwoodie,⁶² M. Ebert,⁶² R. C. Field,⁶²
 B. G. Fulsom,⁶² A. M. Gabareen,⁶² M. T. Graham,⁶² C. Hast,⁶² W. R. Innes,⁶² M. H. Kelsey,⁶² P. Kim,⁶²
 M. L. Kocian,⁶² D. W. G. S. Leith,⁶² P. Lewis,⁶² D. Lindemann,⁶² B. Lindquist,⁶² S. Luitz,⁶² V. Luth,⁶² H. L. Lynch,⁶²
 D. B. MacFarlane,⁶² D. R. Muller,⁶² H. Neal,⁶² S. Nelson,⁶² M. Perl,⁶² T. Pulliam,⁶² B. N. Ratcliff,⁶² A. Roodman,⁶²
 A. A. Salnikov,⁶² R. H. Schindler,⁶² A. Snyder,⁶² D. Su,⁶² M. K. Sullivan,⁶² J. Va'vra,⁶² A. P. Wagner,⁶² W. F. Wang,⁶²
 W. J. Wisniewski,⁶² M. Wittgen,⁶² D. H. Wright,⁶² H. W. Wulsin,⁶² V. Ziegler,⁶² W. Park,⁶³ M. V. Purohit,⁶³
 R. M. White,⁶³ J. R. Wilson,⁶³ A. Randle-Conde,⁶⁴ S. J. Sekula,⁶⁴ M. Bellis,⁶⁵ P. R. Burchat,⁶⁵ T. S. Miyashita,⁶⁵
 E. M. T. Puccio,⁶⁵ M. S. Alam,⁶⁶ J. A. Ernst,⁶⁶ R. Gorodeisky,⁶⁷ N. Guttman,⁶⁷ D. R. Peimer,⁶⁷ A. Soffer,⁶⁷
 S. M. Spanier,⁶⁸ J. L. Ritchie,⁶⁹ A. M. Ruland,⁶⁹ R. F. Schwitters,⁶⁹ B. C. Wray,⁶⁹ J. M. Izen,⁷⁰ X. C. Lou,⁷⁰
 F. Bianchi,^{71a,71b} D. Gamba,^{71a,71b} S. Zambito,^{71a,71b} L. Lanceri,^{72a,72b} L. Vitale,^{72a,72b} F. Martinez-Vidal,⁷³
 A. Oyanguren,⁷³ P. Villanueva-Perez,⁷³ H. Ahmed,⁷⁴ J. Albert,⁷⁴ Sw. Banerjee,⁷⁴ F. U. Bernlochner,⁷⁴ H. H. F. Choi,⁷⁴
 G. J. King,⁷⁴ R. Kowalewski,⁷⁴ M. J. Lewczuk,⁷⁴ I. M. Nugent,⁷⁴ J. M. Roney,⁷⁴ R. J. Sobie,⁷⁴ N. Tasneem,⁷⁴
 T. J. Gershon,⁷⁵ P. F. Harrison,⁷⁵ T. E. Latham,⁷⁵ H. R. Band,⁷⁶ S. Dasu,⁷⁶ Y. Pan,⁷⁶ R. Prepost,⁷⁶ and S. L. Wu⁷⁶

(BABAR Collaboration)

- ¹Laboratoire d'Annecy-le-Vieux de Physique des Particules (LAPP), Université de Savoie, CNRS/IN2P3, F-74941 Annecy-Le-Vieux, France
- ²Departament ECM, Facultat de Física, Universitat de Barcelona, E-08028 Barcelona, Spain
- ^{3a}INFN Sezione di Bari, I-70126 Bari, Italy
- ^{3b}Dipartimento di Fisica, Università di Bari, I-70126 Bari, Italy
- ⁴University of Bergen, Institute of Physics, N-5007 Bergen, Norway
- ⁵Lawrence Berkeley National Laboratory and University of California, Berkeley, California 94720, USA
- ⁶Ruhr Universität Bochum, Institut für Experimentalphysik 1, D-44780 Bochum, Germany
- ⁷University of British Columbia, Vancouver, British Columbia V6T 1Z1, Canada
- ⁸Brunel University, Uxbridge, Middlesex UB8 3PH, United Kingdom
- ⁹Budker Institute of Nuclear Physics SB RAS, Novosibirsk 630090, Russia
- ¹⁰University of California at Irvine, Irvine, California 92697, USA
- ¹¹University of California at Riverside, Riverside, California 92521, USA
- ¹²University of California at Santa Barbara, Santa Barbara, California 93106, USA
- ¹³University of California at Santa Cruz, Institute for Particle Physics, Santa Cruz, California 95064, USA
- ¹⁴California Institute of Technology, Pasadena, California 91125, USA
- ¹⁵University of Cincinnati, Cincinnati, Ohio 45221, USA
- ¹⁶University of Colorado, Boulder, Colorado 80309, USA
- ¹⁷Colorado State University, Fort Collins, Colorado 80523, USA
- ¹⁸Fakultät Physik, Technische Universität Dortmund, D-44221 Dortmund, Germany
- ¹⁹Technische Universität Dresden, Institut für Kern und Teilchenphysik, D-01062 Dresden, Germany
- ²⁰Laboratoire Leprince-Ringuet, Ecole Polytechnique, CNRS/IN2P3, F-91128 Palaiseau, France
- ²¹University of Edinburgh, Edinburgh EH9 3JZ, United Kingdom
- ^{22a}INFN Sezione di Ferrara, I-44100 Ferrara, Italy
- ^{22b}Dipartimento di Fisica, Università di Ferrara, I-44100 Ferrara, Italy
- ²³INFN Laboratori Nazionali di Frascati, I-00044 Frascati, Italy
- ^{24a}INFN Sezione di Genova, I-16146 Genova, Italy
- ^{24b}Dipartimento di Fisica, Università di Genova, I-16146 Genova, Italy
- ²⁵Indian Institute of Technology Guwahati, Guwahati, Assam 781 039, India
- ²⁶Harvard University, Cambridge, Massachusetts 02138, USA
- ²⁷Universität Heidelberg, Physikalisches Institut, Philosophenweg 12, D-69120 Heidelberg, Germany
- ²⁸Humboldt-Universität zu Berlin, Institut für Physik, Newtonstrasse 15, D-12489 Berlin, Germany
- ²⁹Imperial College London, London SW7 2AZ, United Kingdom
- ³⁰University of Iowa, Iowa City, Iowa 52242, USA
- ³¹Iowa State University, Ames, Iowa 50011-3160, USA
- ³²Johns Hopkins University, Baltimore, Maryland 21218, USA
- ³³Laboratoire de l'Accélérateur Linéaire, IN2P3/CNRS et Université Paris-Sud 11, Centre Scientifique d'Orsay, B. P. 34, F-91898 Orsay Cedex, France
- ³⁴Lawrence Livermore National Laboratory, Livermore, California 94550, USA
- ³⁵University of Liverpool, Liverpool L69 7ZE, United Kingdom
- ³⁶Queen Mary, University of London, London E1 4NS, United Kingdom
- ³⁷University of London, Royal Holloway and Bedford New College, Egham, Surrey TW20 0EX, United Kingdom
- ³⁸University of Louisville, Louisville, Kentucky 40292, USA
- ³⁹Johannes Gutenberg-Universität Mainz, Institut für Kernphysik, D-55099 Mainz, Germany
- ⁴⁰University of Manchester, Manchester M13 9PL, United Kingdom
- ⁴¹University of Maryland, College Park, Maryland 20742, USA
- ⁴²University of Massachusetts, Amherst, Massachusetts 01003, USA
- ⁴³Laboratory for Nuclear Science, Massachusetts Institute of Technology, Cambridge, Massachusetts 02139, USA
- ⁴⁴McGill University, Montréal, Québec H3A 2T8, Canada
- ^{45a}INFN Sezione di Milano, I-20133 Milano, Italy
- ^{45b}Dipartimento di Fisica, Università di Milano, I-20133 Milano, Italy
- ⁴⁶University of Mississippi, University, Mississippi 38677, USA
- ⁴⁷Université de Montréal, Physique des Particules, Montréal, Québec H3C 3J7, Canada
- ^{48a}INFN Sezione di Napoli, I-80126 Napoli, Italy
- ^{48b}Dipartimento di Scienze Fisiche, Università di Napoli Federico II, I-80126 Napoli, Italy
- ⁴⁹NIKHEF, National Institute for Nuclear Physics and High Energy Physics, NL-1009 DB Amsterdam, The Netherlands
- ⁵⁰University of Notre Dame, Notre Dame, Indiana 46556, USA

- ⁵¹Ohio State University, Columbus, Ohio 43210, USA
⁵²University of Oregon, Eugene, Oregon 97403, USA
^{53a}INFN Sezione di Padova, I-35131 Padova, Italy
^{53b}Dipartimento di Fisica, Università di Padova, I-35131 Padova, Italy
⁵⁴Laboratoire de Physique Nucléaire et de Hautes Energies, IN2P3/CNRS, Université Pierre et Marie Curie-Paris6, Université Denis Diderot-Paris7, F-75252 Paris, France
^{55a}INFN Sezione di Perugia, I-06100 Perugia, Italy
^{55b}Dipartimento di Fisica, Università di Perugia, I-06100 Perugia, Italy
^{56a}INFN Sezione di Pisa, I-56127 Pisa, Italy
^{56b}Dipartimento di Fisica, Università di Pisa, I-56127 Pisa, Italy
^{56c}Scuola Normale Superiore di Pisa, I-56127 Pisa, Italy
⁵⁷Princeton University, Princeton, New Jersey 08544, USA
^{58a}INFN Sezione di Roma, I-00185 Roma, Italy
^{58b}Dipartimento di Fisica, Università di Roma La Sapienza, I-00185 Roma, Italy
⁵⁹Universität Rostock, D-18051 Rostock, Germany
⁶⁰Rutherford Appleton Laboratory, Chilton, Didcot, Oxon OX11 0QX, United Kingdom
⁶¹Centre de Saclay, CEA, Irfu, SPP, F-91191 Gif-sur-Yvette, France
⁶²SLAC National Accelerator Laboratory, Stanford, California 94309, USA
⁶³University of South Carolina, Columbia, South Carolina 29208, USA
⁶⁴Southern Methodist University, Dallas, Texas 75275, USA
⁶⁵Stanford University, Stanford, California 94305-4060, USA
⁶⁶State University of New York, Albany, New York 12222, USA
⁶⁷School of Physics and Astronomy, Tel Aviv University, Tel Aviv 69978, Israel
⁶⁸University of Tennessee, Knoxville, Tennessee 37996, USA
⁶⁹University of Texas at Austin, Austin, Texas 78712, USA
⁷⁰University of Texas at Dallas, Richardson, Texas 75083, USA
^{71a}INFN Sezione di Torino, I-10125 Torino, Italy
^{71b}Dipartimento di Fisica Sperimentale, Università di Torino, I-10125 Torino, Italy
^{72a}INFN Sezione di Trieste, I-34127 Trieste, Italy
^{72b}Dipartimento di Fisica, Università di Trieste, I-34127 Trieste, Italy
⁷³IFIC, Universitat de Valencia-CSIC, E-46071 Valencia, Spain
⁷⁴University of Victoria, Victoria, British Columbia V8W 3P6, Canada
⁷⁵Department of Physics, University of Warwick, Coventry CV4 7AL, United Kingdom
⁷⁶University of Wisconsin, Madison, Wisconsin 53706, USA

(Received 14 December 2012; published 18 March 2013)

We report a search for CP violation in the decay modes $D^\pm \rightarrow K_S^0 K^\pm$, $D_s^\pm \rightarrow K_S^0 K^\pm$, and $D_s^\pm \rightarrow K_S^0 \pi^\pm$ using a data set corresponding to an integrated luminosity of 469 fb^{-1} collected with the BABAR detector at the PEP-II asymmetric energy e^+e^- storage rings. The decay rate CP asymmetries, A_{CP} , are determined to be $(+0.13 \pm 0.36(\text{stat}) \pm 0.25(\text{syst}))\%$, $(-0.05 \pm 0.23(\text{stat}) \pm 0.24(\text{syst}))\%$, and $(+0.6 \pm 2.0(\text{stat}) \pm 0.3(\text{syst}))\%$, respectively. These measurements are consistent with zero, and also with the Standard Model prediction $[(-0.332 \pm 0.006)\%$ for the $D^\pm \rightarrow K_S^0 K^\pm$ and $D_s^\pm \rightarrow K_S^0 K^\pm$ modes, and $(+0.332 \pm 0.006)\%$ for the $D_s^\pm \rightarrow K_S^0 \pi^\pm$ mode]. They are the most precise determinations to date.

DOI: [10.1103/PhysRevD.87.052012](https://doi.org/10.1103/PhysRevD.87.052012)

PACS numbers: 11.30.Er, 13.25.Ft, 14.40.Lb

I. INTRODUCTION

The search for CP violation (CPV) in charm decays provides a sensitive probe of physics beyond the Standard

Model (SM). Owing to its suppression within the SM, a significant observation of direct CPV in charm decays would indicate the possible presence of new physics effects in the decay processes. In a previous article [1], we reported a precise measurement of the CP asymmetry in the $D^\pm \rightarrow K_S^0 \pi^\pm$ mode, where the measured asymmetry was found to be consistent with the value expected from indirect CPV in the K^0 system.

The LHCb and CDF Collaborations have recently reported evidence for CPV in charm decays by measuring the difference of CP asymmetries in the $D^0 \rightarrow K^+ K^-$ and $D^0 \rightarrow \pi^+ \pi^-$ channels [2,3], which is mainly sensitive to direct CPV . The size of the world average direct CP

*Present address: The University of Tabuk, Tabuk 71491, Saudi Arabia.

†Also at Dipartimento di Fisica, Università di Perugia, Perugia, Italy.

‡Present address: The University of Huddersfield, Huddersfield HD1 3DH, United Kingdom.

§Deceased.

||Present address: University of South Alabama, Mobile, AL 36688, USA.

¶Also at Università di Sassari, Sassari, Italy.

asymmetry difference, $(-6.56 \pm 1.54) \times 10^{-3}$ [4], suggests either a significant enhancement of SM penguin amplitudes or of new physics amplitudes (or both) in charm decays [5]. Improved measurements of the CP asymmetries in the individual two-body modes, along with measurements in other channels, are needed to determine the nature of the contributing amplitudes.

We present herein measurements of the decay rate CP asymmetry, A_{CP} , defined as

$$A_{CP} = \frac{\Gamma(D_{(s)}^+ \rightarrow f) - \Gamma(D_{(s)}^- \rightarrow \bar{f})}{\Gamma(D_{(s)}^+ \rightarrow f) + \Gamma(D_{(s)}^- \rightarrow \bar{f})}, \quad (1)$$

in the decay modes $D^\pm \rightarrow K_S^0 K^\pm$, $D_s^\pm \rightarrow K_S^0 K^\pm$, and $D_s^\pm \rightarrow K_S^0 \pi^\pm$. Previous measurements of A_{CP} in these channels have been reported by the CLEO-c [6] and Belle Collaborations [7]. As for the A_{CP} measurement in $D^\pm \rightarrow K_S^0 \pi^\pm$, we expect an A_{CP} asymmetry of $(\pm 0.332 \pm 0.006)\%$ [8] resulting from CPV in $K^0 - \bar{K}^0$ mixing [9]. The sign of the K^0 -induced asymmetry is positive (negative) if a K^0 (\bar{K}^0) is present in the corresponding tree-level Feynman diagram. Because it is identified by its $\pi^+ \pi^-$ decay, the intermediate state is a coherent mix of K_S^0 and K_L^0 amplitudes. It has been shown in Ref. [10] that the $K_S^0 - K_L^0$ interference term gives rise to a measured CP asymmetry that depends on the range in proper time over which the decay rates are integrated and on the efficiency for the reconstruction of the intermediate state as a function of its proper flight time.

For this analysis we employ a technique similar to that used for our measurement of CPV in the $D^\pm \rightarrow K_S^0 \pi^\pm$ mode [1]. As a result, reference to our previous publication is given for the description of some of the analysis details.

II. THE BABAR DETECTOR AND EVENT SELECTION

The data used for these measurements were recorded at or near the $Y(4S)$ resonance by the *BABAR* detector at the PEP-II storage rings and correspond to an integrated luminosity of 469 fb^{-1} . Charged particles are detected, and their momenta measured, by a combination of a silicon vertex tracker, consisting of five layers of double-sided detectors, and a 40-layer central drift chamber, both operating in a 1.5 T axial magnetic field. Charged-particle identification is provided by specific ionization energy loss measurements in the tracking system and by the measured Cherenkov angle from an internally reflecting ring-imaging Cherenkov detector covering the central region of the detector. Electrons are detected by a CsI(Tl) electromagnetic calorimeter. The *BABAR* detector, and the coordinate system used throughout, are described in detail in Refs. [11,12]. We validate the analysis procedure using Monte Carlo (MC) simulation based on GEANT4 [13]. The MC samples include $e^+ e^- \rightarrow q\bar{q}$ ($q = u, d, s, c$) events, simulated with JETSET [14] and $B\bar{B}$ decays simulated

with the EVTGEN generator [15]. To avoid potential bias in the measurements we finalize the event selection for each channel, as well as the procedures for efficiency correction, fitting, and the determination of the systematic uncertainties and possible biases in the measurements, prior to extracting the value of A_{CP} from the data.

Signal candidates are reconstructed by combining a K_S^0 candidate, reconstructed in the decay mode $K_S^0 \rightarrow \pi^+ \pi^-$, with a charged pion or kaon candidate. A K_S^0 candidate is reconstructed from two oppositely charged tracks with an invariant mass within a $\pm 10 \text{ MeV}/c^2$ interval centered on the nominal K_S^0 mass [8], which is approximately $\pm 2.5\sigma$ in the measured K_S^0 mass resolution. The χ^2 probability of the $\pi^+ \pi^-$ vertex fit must be greater than 0.1%. Motivated by MC studies, we require the measured flight length of the K_S^0 candidate to be at least 3 times greater than its uncertainty, to reduce combinatorial background. A reconstructed charged-particle track that has $p_T \geq 400 \text{ MeV}/c$ is selected as a pion or kaon candidate, where p_T is the magnitude of the momentum in the plane perpendicular to the z axis (transverse plane). In our measurement, we require that a pion candidate not be identified as a kaon, a proton, or an electron, and that a kaon candidate be identified as a kaon, and not as a pion, a proton, or an electron. Identification efficiencies and misidentification rates for electron, pions, kaons, and protons with $2 \text{ GeV}/c$ momentum in the laboratory frame are reported in Table I. The criteria used to select pion or kaon candidates are very effective in reducing the charge asymmetry from track reconstruction and identification, as inferred from studying the data control samples described below. A vertex fit to the whole decay chain, constraining the $D_{(s)}^\pm$ production vertex to be within the $e^+ e^-$ interaction region, is then performed [16]. We retain only $D_{(s)}^\pm$ candidates having a χ^2 probability for this fit greater than 0.1%, and an invariant mass $m(K_S^0 h)$, $h = \pi, K$, within a $\pm 65 \text{ MeV}/c^2$ interval centered on the nominal $D_{(s)}^\pm$ mass [8], which is approximately equivalent to $\pm 8\sigma$ in the measured $D_{(s)}^\pm$ mass resolution.

TABLE I. Identification efficiencies and misidentification rates for electron, pions, kaons, and protons with $2 \text{ GeV}/c$ momentum in the laboratory frame. The values for kaons on the third row refers to the identification criterion used to reject kaons from the pion sample, while the values on the fourth row to the criterion used in the kaon selection.

Particle	Efficiency [%]	Misidentification rate [%]	
		π^\pm	K^\pm
e^\pm	91	0.04	<0.2
π^\pm	88	not applicable	1
K^\pm (applied to π^\pm)	91	1	not applicable
K^\pm (applied to K^\pm)	99	8	not applicable
p^\pm	80	0.2	0.2

We require further that the magnitude of the D_s^\pm candidate momentum in the e^+e^- center-of-mass system, p^* , be between 2.6 and 5.0 GeV/ c , in order to suppress combinatorial background from $B\bar{B}$ events. For the $D^\pm \rightarrow K_S^0 K^\pm$ mode, the MC simulated sample shows that retaining candidates with p^* between 2.0 and 5.0 GeV/ c allows signal candidates from B -meson decays, without introducing an excessive amount of combinatorial background. Assuming that CPT is conserved, there is no contribution to A_{CP} from CP violation in B meson decays from Standard Model processes. Additional background rejection is obtained by requiring that the impact parameter of the $D_{(s)}^\pm$ candidate with respect to the beam spot [11], projected onto the transverse plane, be less than 0.3 cm, and that the $D_{(s)}^\pm$ proper decay time, t_{xy} , be between -15 and 35 ps. The decay time is measured using L_{xy} , defined as the distance of the $D_{(s)}^\pm$ decay vertex from the beam spot projected onto the transverse plane.

In order to further optimize the sensitivity of the A_{CP} measurements, we construct a multivariate algorithm, based on seven discriminating variables for each $D_{(s)}^\pm$ candidate: t_{xy} , L_{xy} , p^* , the momentum magnitude and component in the transverse plane for the K_S^0 candidate, and also for the pion or kaon candidate. For the $D^\pm \rightarrow K_S^0 K^\pm$ and $D_s^\pm \rightarrow K_S^0 K^\pm$ modes the multivariate algorithm with the best performance is a boosted decision tree [17], while for the $D_s^\pm \rightarrow K_S^0 \pi^\pm$ mode the best algorithm is a projective likelihood method [17]. The final selection criteria, based on the outputs of the multivariate selectors, are optimized using truth-matched signal and background candidates from the MC sample. For the optimization, we maximize the $S/\sqrt{S+B}$ ratio, where S and B are the numbers of signal and background candidates, respectively, with invariant mass within ± 30 MeV/ c^2 of the nominal $D_{(s)}^\pm$ mass, which is approximately $\pm 3\sigma$ in the measured mass resolution.

III. SIGNAL YIELD AND ASYMMETRY EXTRACTION

For each mode the signal yield is extracted using a binned maximum likelihood (ML) fit to the distribution of the invariant mass $m(K_S^0 h)$ for the selected $D_{(s)}^\pm$ candidates. The total probability density function (PDF) is the sum of signal and background components. The signal PDF is modeled as a sum of two Gaussian functions for the $D_{(s)}^\pm \rightarrow K_S^0 K^\pm$ modes, and as a single Gaussian function for the $D_s^\pm \rightarrow K_S^0 \pi^\pm$ mode. The background PDF is taken as the sum of two components: a distribution describing the invariant mass of misreconstructed charm meson decays, and a combinatorial background modeling the mass distribution from other sources. For the $D^\pm \rightarrow K_S^0 K^\pm$ ($D_s^\pm \rightarrow K_S^0 \pi^\pm$) mode the charm background is mainly from the tail of the invariant mass distribution for $D_s^\pm \rightarrow K_S^0 K^\pm$ ($D^\pm \rightarrow K_S^0 \pi^\pm$) candidates. For the $D_s^\pm \rightarrow K_S^0 K^\pm$ mode, the misreconstructed charm background originates mainly from $D^\pm \rightarrow K_S^0 \pi^\pm$ decays for which the π^\pm is misidentified as a K^\pm . Assigning the wrong mass to the pion shifts the reconstructed invariant mass, and the resulting distribution is a broad peak with mean value close to the D_s^\pm mass. For each mode, the invariant mass distribution due to charm background is modeled using a histogram PDF obtained from a MC sample of simulated charm background decays. The combinatorial background is described by a first(second)-order polynomial for the $D_s^\pm \rightarrow K_S^0 \pi^\pm$ mode ($D^\pm \rightarrow K_S^0 K^\pm$ and $D_s^\pm \rightarrow K_S^0 K^\pm$ modes). The fits to the $m(K_S^0 h)$ distributions yield $(159.4 \pm 0.8) \times 10^3$ $D^\pm \rightarrow K_S^0 K^\pm$ decays, $(288.2 \pm 1.1) \times 10^3$ $D_s^\pm \rightarrow K_S^0 K^\pm$ decays, and $(14.33 \pm 0.31) \times 10^3$ $D_s^\pm \rightarrow K_S^0 \pi^\pm$ decays. The data and the fit results are shown in Fig. 1. All of the PDF parameters are extracted from fits to the data.

For each channel, we determine A_{CP} by measuring the signal yield asymmetry A defined as

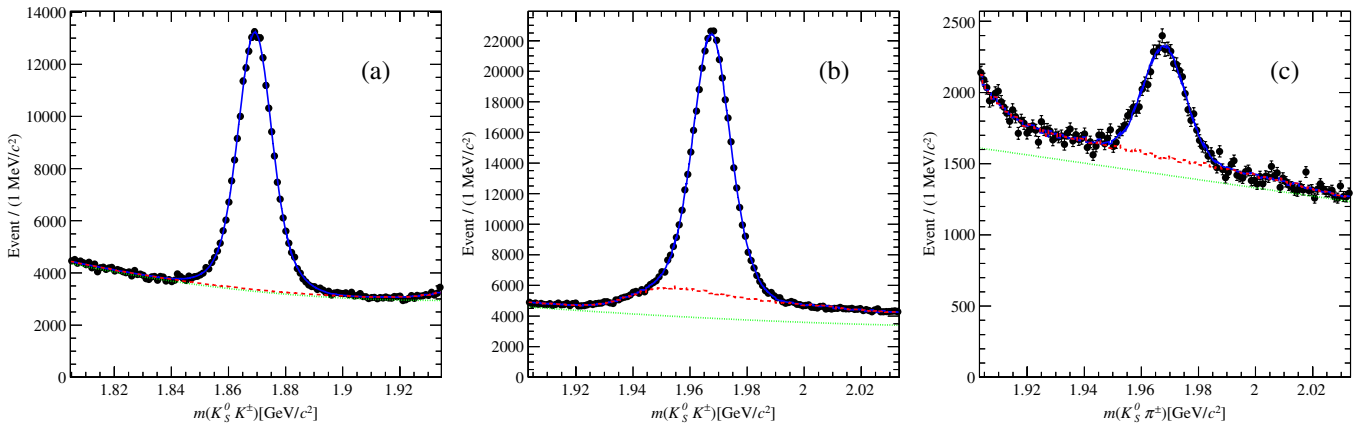


FIG. 1 (color online). Invariant mass distribution for (a) $D^\pm \rightarrow K_S^0 K^\pm$, (b) $D_s^\pm \rightarrow K_S^0 K^\pm$, and (c) $D_s^\pm \rightarrow K_S^0 \pi^\pm$ candidates (points with error bars). The solid curve shows the result of the fit to the data. The dashed curve represents the sum of all background contributions, while the dotted curve indicates combinatorial background only.

$$A = \frac{N_{D_{(s)}^+} - N_{D_{(s)}^-}}{N_{D_{(s)}^+} + N_{D_{(s)}^-}}, \quad (2)$$

where $N_{D_{(s)}^+}$ ($N_{D_{(s)}^-}$) is the number of $D_{(s)}^+$ ($D_{(s)}^-$) decays determined from the fit to the invariant mass distribution. The asymmetry A contains two contributions in addition to A_{CP} , namely the forward-backward (FB) asymmetry (A_{FB}), and a detector-induced component. We measure A_{FB} together with A_{CP} using the selected data set, while we correct the data for the detector-induced component using coefficients derived from a control sample.

IV. CORRECTION OF DETECTOR-RELATED ASYMMETRIES

We use a data-driven method, described in detail in Ref. [1], to determine the charge asymmetry in track reconstruction as a function of the magnitude of the track momentum and its polar angle in the laboratory frame. The method exploits the fact that $Y(4S) \rightarrow B\bar{B}$ events provide a sample evenly populated with positive and negative tracks, free of any physics-induced asymmetries. The off-resonance momentum distribution is subtracted from the on-resonance one, to remove any contribution from continuum, for which there is a FB asymmetry in the center-of-mass frame. This sample is used to compute the detector-related asymmetries in the reconstruction of charged-particle tracks. Starting from a sample of 50.6 fb^{-1} of data collected at the $Y(4S)$ resonance and an off-resonance data sample of 44.8 fb^{-1} , we obtain a large sample of charged-particle tracks and apply the same charged pion or kaon track selection criteria used in the reconstruction of the $D_{(s)}^\pm \rightarrow K_S^0 K^\pm$ and $D_s^\pm \rightarrow K_S^0 \pi^\pm$ modes. Then, after subtracting the off-resonance contribution from the on-resonance sample, we obtain a sample of more than 120×10^6 pion candidates, and 40×10^6 kaon candidates, originating from $Y(4S)$ decays. We use the full off-resonance sample and an equivalent luminosity for the on-resonance sample, because, due to the subtraction procedure, including additional data in the on-resonance sample does not improve the statistical error on the correction ratios mentioned below. These candidates are then used to compute the efficiency ratios for positive and negative pions and kaons. The ratio values and their statistical errors for pions and kaons are shown in Figs. 2 and 3, respectively. For the $D_{(s)}^- \rightarrow K_S^0 K^-$ ($D_s^- \rightarrow K_S^0 \pi^-$) modes, the $D_{(s)}^-$ (D_s^-) yields, in intervals of kaon (pion) momentum and cosine of its polar angle, $\cos \theta$, are weighted with the kaon (pion) efficiency ratios to correct for the detection efficiency differences between K^+ and K^- (π^+ and π^-). Momentum and cosine of its polar angle intervals are not uniform in order to have similar statistics, and therefore similar correction uncertainty, in each interval. Interval sizes vary from (0.05 GeV/c, 0.06) to (4.4 GeV/c, 0.96), where the first number is the momentum interval, and the

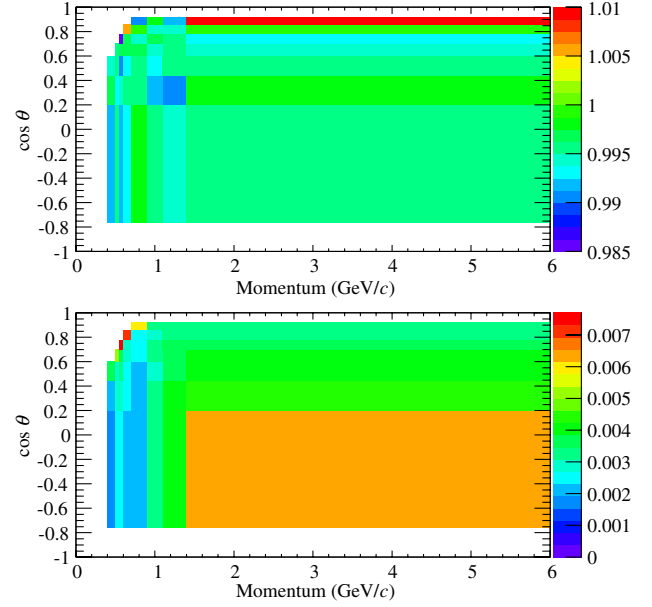


FIG. 2 (color online). (Top) The ratio between the detection efficiency for π^+ and π^- , and (bottom) the corresponding statistical errors. The values are computed using the numbers of π^+ and π^- tracks in the selected control sample.

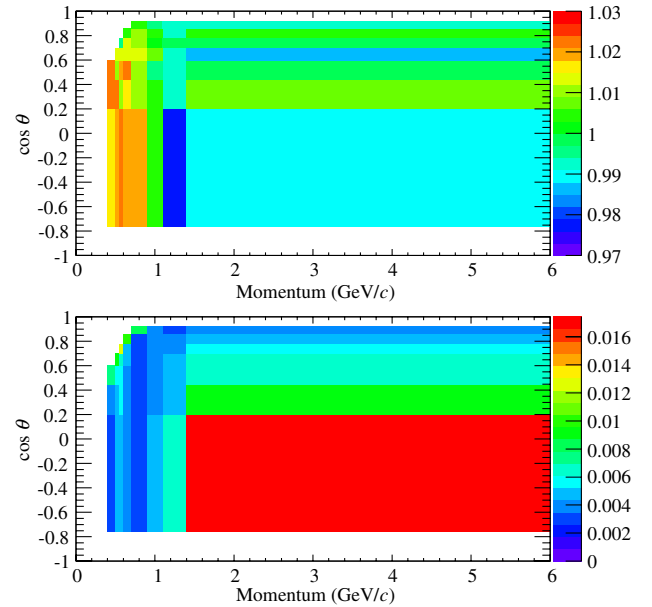


FIG. 3 (color online). (Top) The ratio between the detection efficiency for K^+ and K^- , and (bottom) the corresponding statistical errors. The values are computed using the numbers of K^+ and K^- tracks in the selected control sample.

second its cosine of polar angle interval. The largest correction is approximately 1% for pions and 2% for kaons. After correcting the data for the detector-induced component only A_{FB} and A_{CP} contribute to the measured asymmetry A .

V. EXTRACTION OF A_{CP} AND A_{FB}

Neglecting higher-order terms that contain A_{CP} and A_{FB} , the resulting asymmetry can be expressed simply as the sum of the two. Given that A_{FB} is an odd function of $\cos \theta_D^*$, where θ_D^* is the polar angle of the $D_{(s)}^\pm$ candidate momentum in the center-of-mass frame, A_{CP} and A_{FB} can be written as a function of $|\cos \theta_D^*|$ as follows:

$$A_{CP}(|\cos \theta_D^*|) = \frac{A(+|\cos \theta_D^*|) + A(-|\cos \theta_D^*|)}{2} \quad (3)$$

and

$$A_{FB}(|\cos \theta_D^*|) = \frac{A(+|\cos \theta_D^*|) - A(-|\cos \theta_D^*|)}{2}, \quad (4)$$

where $A(+|\cos \theta_D^*|)$ [$A(-|\cos \theta_D^*|)$] is the measured asymmetry for the $D_{(s)}^\pm$ candidates in a positive (negative) $\cos \theta_D^*$ interval.

A simultaneous ML fit to the $D_{(s)}^+$ and $D_{(s)}^-$ invariant mass distributions is carried out to extract the signal yield asymmetry in each of ten equally spaced $\cos \theta_D^*$ intervals, starting with interval 1 at $[-1.0, -0.8]$. The PDF model that describes the distribution in each subsample is the same as that used in the fit to the full sample, but the

following parameters are allowed to float separately in each subsample (referred to as split parameters): the yields for signal, charm background and combinatorial candidates; the asymmetries for signal and combinatorial candidates; the width, and the fraction of the Gaussian function with the larger contribution to the signal PDF; and the first-order coefficient of the polynomial that models the combinatorial background. For the $D^\pm \rightarrow K_S^0 K^\pm$ mode the yields for the charm background candidates in intervals 1, 2, and 3 were fixed to 0 to obtain a fully convergent fit. Since interval 10 contains the smallest number of candidates, we use a single Gaussian function to model the signal PDF for the $D_{(s)}^\pm \rightarrow K_S^0 K^\pm$ modes. For the CP asymmetry of charm background candidates we use the same floating parameters as for the signal candidates, because the largest source of CP asymmetry for both samples is due to CPV in $K^0 - \bar{K}^0$ mixing. For the $D_s^\pm \rightarrow K_S^0 \pi^\pm$ mode, where the primary charm background channel, $D^\pm \rightarrow K_S^0 \pi^\pm$, has the same magnitude but opposite-sign asymmetry due to $K^0 - \bar{K}^0$ mixing, we use a separate parameter for the asymmetry of the charm background candidates. To achieve a more stable fit, if the fit results for a split parameter are statistically compatible between two or more subsamples, the parameter is forced to have the same floating value among those subsamples only. For the $D_s^\pm \rightarrow K_S^0 \pi^\pm$ mode the width of the

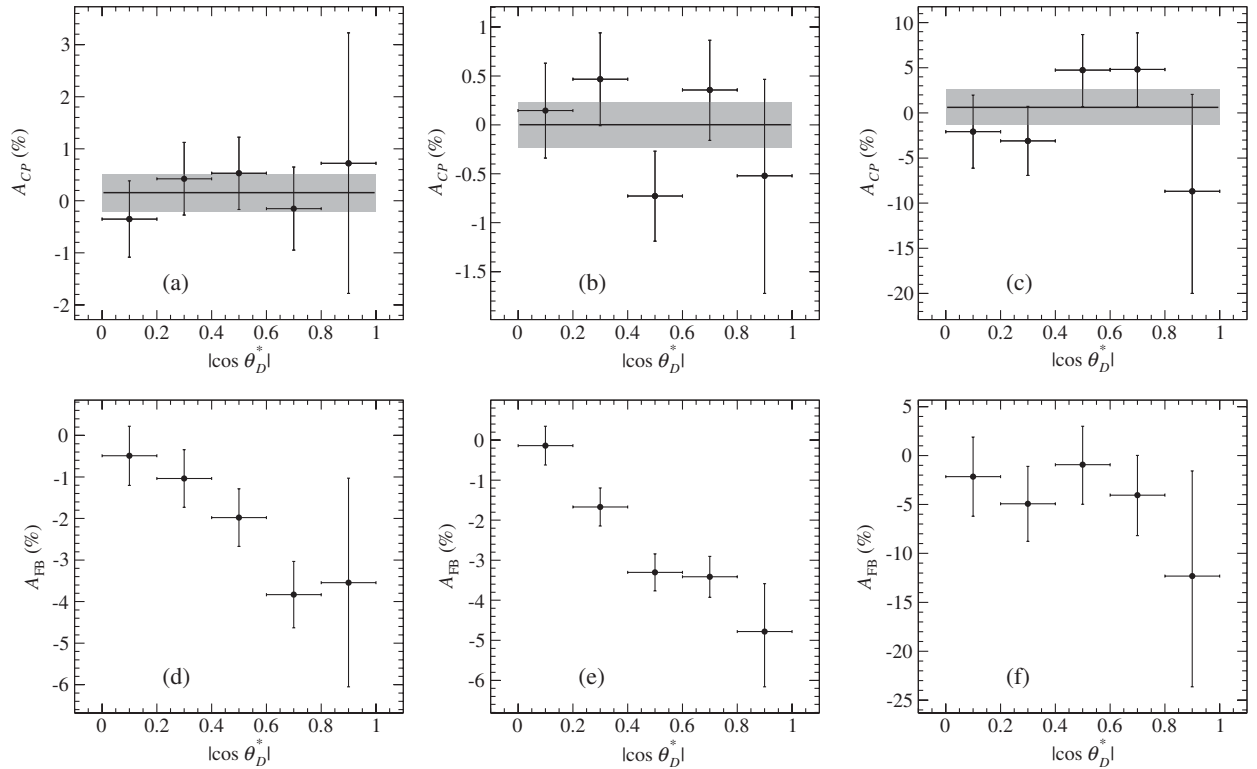


FIG. 4. CP asymmetry, A_{CP} , for (a) $D^\pm \rightarrow K_S^0 K^\pm$, (b) $D_s^\pm \rightarrow K_S^0 K^\pm$, and (c) $D_s^\pm \rightarrow K_S^0 \pi^\pm$ as a function of $|\cos \theta_D^*|$ in the data sample. The solid line represents the central value of A_{CP} and the gray band is the $\pm 1\sigma$ interval, both obtained from a χ^2 minimization assuming no dependence on $|\cos \theta_D^*|$. The corresponding forward-backward asymmetries, A_{FB} , are shown in (d)–(f).

first Gaussian function for the signal PDF is set to the same floating value in intervals 1, 2, 3, and 4. The first-order coefficient of the polynomial describing the combinatorial background is set to the same floating value in intervals 4–8 ($D^\pm \rightarrow K_S^0 K^\pm$), in intervals 4–8 ($D_s^\pm \rightarrow K_S^0 K^\pm$), and in intervals 2–7 ($D_s^\pm \rightarrow K_S^0 \pi^\pm$). The final fit contains 70, 80, and 64 free parameters for the $D^\pm \rightarrow K_S^0 K^\pm$, $D_s^\pm \rightarrow K_S^0 K^\pm$, and $D_s^\pm \rightarrow K_S^0 \pi^\pm$ modes, respectively.

The A_{CP} and A_{FB} values for the five $|\cos \theta_D^*|$ bins are shown in Fig. 4 for the three decay modes. The weighted average of the five A_{CP} values is $(0.16 \pm 0.36)\%$ for the $D^\pm \rightarrow K_S^0 K^\pm$ mode, $(0.00 \pm 0.23)\%$ for $D_s^\pm \rightarrow K_S^0 K^\pm$, and $(0.6 \pm 2.0)\%$ for $D_s^\pm \rightarrow K_S^0 \pi^\pm$, where the errors are statistical only.

We perform two tests to validate the analysis procedure for each channel. The first involves generating 5000 toy MC experiments with a statistics equal to data using the PDF and the parameters obtained from the fit to data. After extracting A_{CP} from each experiment, for the $D^\pm \rightarrow K_S^0 K^\pm$ and $D_s^\pm \rightarrow K_S^0 K^\pm$ modes, we deduce from the mean of the A_{CP} pull distributions the presence of a small bias in the fitted value of each fit parameter (the means are -0.036 ± 0.014 and $+0.041 \pm 0.014$, respectively). To account for this effect we apply a correction to the final values equal to $+0.013\%$ for the $D^\pm \rightarrow K_S^0 K^\pm$ mode, and -0.01% for the $D_s^\pm \rightarrow K_S^0 K^\pm$ mode. The A_{CP} pull distributions show that the fit provides an accurate estimate of the statistical error for all the modes. The second test involves fitting a large number of MC events from the full BABAR detector simulation. We measure A_{CP} from this MC sample to be consistent with the generated value of zero.

VI. SYSTEMATICS

The main sources of systematic uncertainty are listed in Table II for each decay mode, together with the overall uncertainties. The primary sources of systematic uncertainty are the detection efficiency ratios used to weight the $D_{(s)}^-$ yields, and the contributions from misidentified particles in the data control sample used to determine the charge asymmetry in track reconstruction efficiency.

The technique used to remove the charge asymmetry due to detector-induced effects produces a small systematic uncertainty in the measurement of A_{CP} due to the statistical error in the relative efficiency estimation. This systematic uncertainty depends only on the type of charged particle (pion or kaon) in the final state, and not on the initial state. To estimate the systematic uncertainty on A_{CP} resulting from this source, the relative charged-particle efficiency in each interval of momentum and $\cos \theta$ is randomly drawn from a Gaussian distribution whose mean is the nominal relative efficiency in that interval, and where the root-mean-squared (rms) deviation is the corresponding statistical error. For each mode, we generate 500 such charged-particle relative-efficiency distributions and use them to obtain 500 A_{CP} values, following the procedure described earlier to determine the nominal value of A_{CP} . The rms deviation of these 500 values from the nominal A_{CP} is taken to be the systematic uncertainty. For the $D_{(s)}^\pm \rightarrow K_S^0 K^\pm$ modes, the estimated systematic uncertainty is 0.23%. For the $D_s^\pm \rightarrow K_S^0 \pi^\pm$ mode, we assign the same systematic uncertainty, 0.06%, as that estimated for the $D^\pm \rightarrow K_S^0 \pi^\pm$ mode in Ref. [1].

The small fraction of misidentified particles in the generic track sample can introduce small biases in the estimation of the efficiencies, and subsequently in the A_{CP} measurements. Because of the good agreement between data and MC samples, we can use the simulated MC candidates to measure the shift in the A_{CP} value from the fit when the corrections are applied, and when they are not. Again, this contribution depends only on the type of the charged-particle track. Hence, for the $D_s^\pm \rightarrow K_S^0 \pi^\pm$ mode, we assume the same shift obtained in Ref. [1], namely $+0.05\%$. By fitting the $D_s^\pm \rightarrow K_S^0 K^\pm$ MC sample when the corrections are applied, and again when not, we obtain a shift of $+0.05\%$ and we assume this for both the $D_s^\pm \rightarrow K_S^0 K^\pm$ and $D^\pm \rightarrow K_S^0 K^\pm$ modes. For all the modes, we shift the measured A_{CP} by this correction value and then, conservatively, include the magnitude of this shift as a contribution to the systematic uncertainty.

Using MC simulation, we evaluate an additional systematic uncertainty of $\pm 0.01\%$ due to a possible charge asymmetry present in the control sample before applying the

TABLE II. Summary of the systematic uncertainty contributions for the A_{CP} measurement in each mode. The values are absolute uncertainties, even though given as percentages. The total value corresponds to the sum in quadrature of the individual contributions.

Systematic uncertainty	$D^\pm \rightarrow K_S^0 K^\pm$ [%]	$D_s^\pm \rightarrow K_S^0 K^\pm$ [%]	$D_s^\pm \rightarrow K_S^0 \pi^\pm$ [%]
Efficiency of particle-identification selectors	0.05	0.05	0.05
Statistics of the control sample	0.23	0.23	0.06
Misidentified tracks in the control sample	0.01	0.01	0.01
$\cos \theta_D^*$ interval size	0.04	0.02	0.27
$K^0 - \bar{K}^0$ regeneration	0.05	0.05	0.06
$K_S^0 - K_L^0$ interference	0.015	0.014	0.008
Total	0.25	0.24	0.29

TABLE III. Summary of the A_{CP} measurements. Where reported, the first uncertainty is statistical, and the second is systematic.

	$D^\pm \rightarrow K_S^0 K^\pm$	$D_s^\pm \rightarrow K_S^0 K^\pm$	$D_s^\pm \rightarrow K_S^0 \pi^\pm$
A_{CP} value from the fit	$(+0.155 \pm 0.360)\%$	$(0.00 \pm 0.23)\%$	$(+0.6 \pm 2.0)\%$
Correction for the bias from toy MC experiments	$+0.013\%$	-0.01%	not applied
Correction for the bias in the particle-identification selectors	-0.05%	-0.05%	-0.05%
Correction for the $K_S^0 - K_L^0$ interference (ΔA_{CP})	$+0.015\%$	$+0.014\%$	-0.008%
A_{CP} final value	$(+0.13 \pm 0.36 \pm 0.25)\%$	$(-0.05 \pm 0.23 \pm 0.24)\%$	$(+0.6 \pm 2.0 \pm 0.3)\%$
A_{CP} contribution from $K^0 - \bar{K}^0$ mixing	$(-0.332 \pm 0.006)\%$	$(-0.332 \pm 0.006)\%$	$(+0.332 \pm 0.006)\%$
A_{CP} final value (charm only)	$(+0.46 \pm 0.36 \pm 0.25)\%$	$(+0.28 \pm 0.23 \pm 0.24)\%$	$(+0.3 \pm 2.0 \pm 0.3)\%$

selection criteria. Another source of systematic uncertainty is due to the choice of the $\cos \theta_D^*$ interval size in the simultaneous ML fit. The systematic uncertainty is taken to be the largest absolute difference between the nominal A_{CP} extracted using ten $\cos \theta_D^*$ intervals and that obtained when the fit is performed using either 8 or 12 intervals in $\cos \theta_D^*$. This is the dominant source of systematic uncertainty for the $D_s^\pm \rightarrow K_S^0 \pi^\pm$ mode, as shown in Table II.

We also consider a possible systematic uncertainty due to the regeneration of neutral kaons in the material of the detector. The K^0 and \bar{K}^0 mesons produced in the decay processes can interact with the material in the tracking volume before they decay. Following a method similar to that described in Ref. [18], we compute the probability for a K^0 or a \bar{K}^0 meson to interact inside the *BABAR* tracking system and estimate systematic uncertainties of 0.05% ($D_{(s)}^\pm \rightarrow K_S^0 K^\pm$) and 0.06% ($D_s^\pm \rightarrow K_S^0 \pi^\pm$).

Although the intermediate state is labeled as a K_S^0 , we apply a correction term to the measured A_{CP} to include the effect of $K_S^0 - K_L^0$ interference in the intermediate state [19]. This correction term depends on the proper time range over which decay distributions are integrated, and on the efficiency of the reconstruction of the $\pi^+ \pi^-$ final state as a function of proper time. We compute the reconstruction efficiency distribution as a function of proper time using MC truth-matched K_S^0 decays after the full selection. Following the method in Ref. [19] we estimate the asymmetry-correction term ΔA_{CP} defined as

$$\Delta A_{CP} = A_{CP}^{\text{corr}} - A_{CP}^{\text{fit}}, \quad (5)$$

where A_{CP}^{fit} is the value obtained from the fit and A_{CP}^{corr} is the corrected value. The correction terms are reported in Table III and, to be conservative, we include their absolute values as contributions to the systematic uncertainty estimates. We also estimate the correction factor for the $D^\pm \rightarrow K_S^0 \pi^\pm$ mode using the K_S^0 reconstruction efficiency distribution after the selection detailed in Ref. [1] and obtain the value $+0.002\%$. All these corrections are rather small, even compared to those estimated in a similar analysis [20]. The smaller values of the corrections in the present analysis are due to the improved efficiency for K_S^0

mesons with short decay times that we obtain by applying the requirement on the decay length divided by its uncertainty, rather than on the decay length alone.

VII. CONCLUSION

In conclusion, we measure the direct CP asymmetry A_{CP} in the $D^\pm \rightarrow K_S^0 K^\pm$, $D_s^\pm \rightarrow K_S^0 K^\pm$, and $D_s^\pm \rightarrow K_S^0 \pi^\pm$ modes using approximately 159000, 288000, and 14000 signal candidates, respectively. The measured A_{CP} value for each mode is reported in Table III, where the first errors are statistical and the second are systematic. In the last row of the table, we also report the A_{CP} values after subtracting the expected A_{CP} contribution for each mode due to $K^0 - \bar{K}^0$ mixing. The results are consistent with zero, and with the SM prediction, within 1 standard deviation.

ACKNOWLEDGMENTS

We are grateful for the extraordinary contributions of our PEP-II colleagues in achieving the excellent luminosity and machine conditions that have made this work possible. The success of this project also relies critically on the expertise and dedication of the computing organizations that support *BABAR*. The collaborating institutions wish to thank SLAC for its support and the kind hospitality extended to them. This work is supported by the U.S. Department of Energy and National Science Foundation, the Natural Sciences and Engineering Research Council (Canada), the Commissariat à l'Énergie Atomique and Institut National de Physique Nucléaire et de Physique des Particules (France), the Bundesministerium für Bildung und Forschung and Deutsche Forschungsgemeinschaft (Germany), the Istituto Nazionale di Fisica Nucleare (Italy), the Foundation for Fundamental Research on Matter (Netherlands), the Research Council of Norway, the Ministry of Education and Science of the Russian Federation, Ministerio de Ciencia e Innovación (Spain), and the Science and Technology Facilities Council (United Kingdom). Individuals have received support from the Marie-Curie IEF program (European Union) and the A. P. Sloan Foundation (USA).

- [1] P. del Amo Sanchez *et al.* (BABAR Collaboration), *Phys. Rev. D* **83**, 071103(R) (2011).
- [2] R. Aaij *et al.* (LHCb Collaboration), *Phys. Rev. Lett.* **108**, 111602 (2012).
- [3] T. Aaltonen *et al.* (CDF Collaboration), *Phys. Rev. Lett.* **109**, 111801 (2012).
- [4] Y. Amhis *et al.* (Heavy Flavor Averaging Group), [arXiv:1207.1158](https://arxiv.org/abs/1207.1158); for a more recent update see <http://www.slac.stanford.edu/xorg/hfag/>.
- [5] G. Isidori, J. F. Kamenik, Z. Ligeti, and G. Perez, *Phys. Lett. B* **711**, 46 (2012); H.-Y. Cheng and C.-W. Chiang, *Phys. Rev. D* **85**, 034036 (2012); **85**, 079903(E) (2012); B. Bhattacharya, M. Gronau, and J. L. Rosner, *Phys. Rev. D* **85**, 054014 (2012); G. F. Giudice, G. Isidori, and P. Paradisi, *J. High Energy Phys.* **04** (2012) 060; E. Franco, S. Mishima, and L. Silvestrini, *J. High Energy Phys.* **05** (2012) 140; J. Brod, Y. Grossman, A. L. Kagan, and J. Zupan, *J. High Energy Phys.* **10** (2012) 161.
- [6] S. Dobbs *et al.* (CLEO Collaboration), *Phys. Rev. D* **76**, 112001 (2007).
- [7] B. R. Ko *et al.* (Belle Collaboration), *Phys. Rev. Lett.* **104**, 181602 (2010).
- [8] K. Nakamura (Particle Data Group), *J. Phys. G* **37**, 075021 (2010).
- [9] H. J. Lipkin and Z.-z. Xing, *Phys. Lett. B* **450**, 405 (1999).
- [10] Y. I. Azimov and A. A. Iogansen, *Sov. J. Nucl. Phys.* **33**, 205 (1981).
- [11] B. Aubert *et al.* (BABAR Collaboration), *Nucl. Instrum. Methods Phys. Res., Sect. A* **479**, 1 (2002).
- [12] W. Menges, *IEEE Nucl. Sci. Symp. Conf. Rec.* **3**, 1470 (2006).
- [13] S. Agostinelli *et al.* (Geant4 Collaboration), *Nucl. Instrum. Methods Phys. Res., Sect. A* **506**, 250 (2003).
- [14] T. Sjostrand, S. Mrenna, and P. Z. Skands, *J. High Energy Phys.* **05** (2006) 026.
- [15] D. J. Lange, *Nucl. Instrum. Methods Phys. Res., Sect. A* **462**, 152 (2001).
- [16] W. D. Hulsbergen, *Nucl. Instrum. Methods Phys. Res., Sect. A* **552**, 566 (2005).
- [17] P. Speckmayer, A. Höcker, J. Stelzer, and H. Voss, *J. Phys. Conf. Ser.* **219**, 032057 (2010).
- [18] B. R. Ko, E. Won, B. Golob, and P. Pakhlov, *Phys. Rev. D* **84**, 111501(R) (2011).
- [19] Y. Grossman and Y. Nir, *J. High Energy Phys.* **04** (2012) 002.
- [20] J. P. Lees *et al.* (BABAR Collaboration), *Phys. Rev. D* **85**, 031102(R) (2012); **85**, 099904(E) (2012).